Multiple input describing function analysis
of non-classical aileron buzz

Muhammad I. Zafar[*], Francesca Fusi[a] and Giuseppe Quaranta[b]

Dipartimento di Scienze e Tecnologie Aerospaziali, Politecnico di Milano,
Campus Bovisa Sud, via La Masa, 34, 20165 – Milano, Italy

Abstract. This paper focuses on the computational study of nonlinear effects of unsteady aerodynamics for non-classical aileron buzz. It aims at a comprehensive investigation of the aileron buzz phenomenon under varying flow parameters using the describing function technique with multiple inputs. The limit cycle oscillatory behavior of an asymmetrical airfoil is studied initially using a CFD-based numerical model and direct time marching. Sharp increases in limit cycle amplitude for varying Mach numbers and angles of attack are investigated. An aerodynamic describing function is developed in order to estimate the variation of limit cycle amplitude and frequency with Mach number and angle of attack directly, without time marching. The describing function results are compared to the amplitudes and frequencies predicted by the CFD calculations for validation purposes. Furthermore, a limited sensitivity analysis is presented to demonstrate the potential of the approach for aeroelastic design.

Keywords: computational aeroelasticity; describing function; aileron buzz; fluid structure interaction; limit cycle oscillation

1. Introduction

The transonic flight regime inherently involves nonlinear flow phenomena due to the simultaneous presence of local subsonic and supersonic regions, which can cause shock waves and shock-induced separation. These flow phenomena present various challenging aeroelastic problems that need to be tackled for the design of more efficient and safer aircrafts. Interaction of flow with structural motion leads to the spatial variation of shock wave positions and unsteady flow separation points. For small perturbations about the steady flow, the flow variables and shock wave positions vary in a linear fashion with the wing or control surface motion. However, when the wing or control surface motion is large enough, resulting in large variation of shock waves position or separation of boundary layer, the linear assumption cannot be considered correct. In these conditions the unsteady aerodynamic forces exhibit nonlinear behavior.

The non-linear interaction of control surface motion caused by shock oscillation and unsteady

---

[*]Corresponding author, Graduate Student, E-mail: zafar.muhammad@mail.polimi.it
[a]Ph.D. Student, E-mail: francesca.fusi@polimi.it
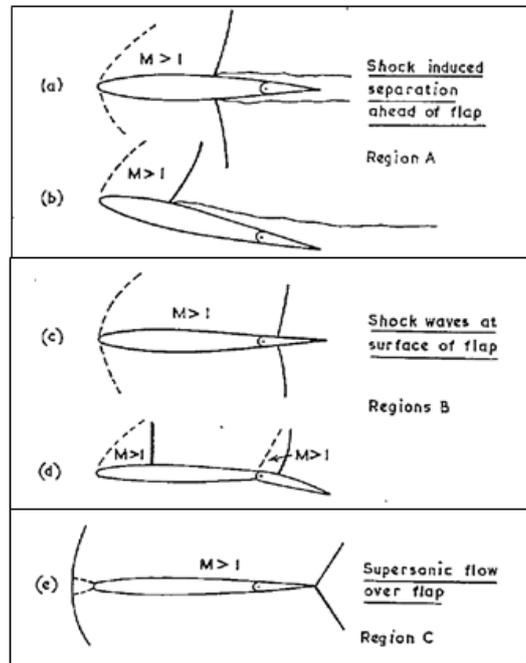[b]Associate Professor, E-mail: giuseppe.quaranta@polimi.it

Fig. 1 Buzz related flow regimes (Lambourne 1962)

flow separation is referred to as *buzz*. Aileron buzz is a single degree of freedom flutter phenomenon involving self-excited oscillations of the aileron about its hinge. Aileron buzz, being an exception among few single degree-of-freedom instabilities, may result in explosive flutter with very large amplitudes within a few cycles and which, in some tests, have led to permanent damage to the aileron and/or wing involved in the flight tests or experiments (Saito 1959, Lambourne 1958). In other cases, it results in small amplitude Limit Cycle Oscillations (LCO), which may cause fatigue damage to the aircraft structure.

For viscous flows, aileron buzz was classified by Lambourne (1962) as Type A, B and C, on the basis of the shock wave location and corresponding mechanisms of buzz excitation. This classification is sketched in Fig. 1. With respect to Type B, Lambourne explained that boundary layer separation was observed, but it did not appear to be the driving mechanism, which it was for Type A buzz. A later work by Bendiksen (1993) endorsed the idea that in such conditions buzz is driven by the dynamics of shock wave motion over the aileron surface. This type of buzz is called *non-classical aileron buzz* to emphasize the occurrence of instability even in the case when boundary layer separation and shock-boundary layer interaction are not determinant.

The development of accurate and efficient models to investigate nonlinear phenomena like aileron buzz involving unsteady aerodynamics has been a focus of research for years. If flight tests demonstrate that an aircraft is susceptible to such oscillations, redesign must take place, which is an extremely expensive process. This was the case for instance for the inboard aileron of the recently developed Boeing 747-8[*], just to report the last known occurrence of this kind of phenomenon. Numerical simulations using Computational Fluid Dynamics (CFD) codes coupled

---

[*]See the web page https://en.wikipedia.org/wiki/Boeing_747-8, accessed in March 2016

with an appropriate structural model have proven to be accurate enough to analyze nonlinearities involved in the unsteady aerodynamics of aileron buzz (Steger and Bailey 1980, Fuglsang *et al*. 1992, Bendiksen 1993, Pak and Baker 2001, Fusi *et al*. 2012, Forestieri *et al*. 2011, Gao *et al*. 2015). However, standard CFD models that include the relevant aerodynamic nonlinearities are too expensive, especially if developed for parametric design analysis to be performed in the preliminary design phases of aircraft development. Thus, there has been much interest in reducing computational costs while retaining the essence of the nonlinear flow phenomenon.

Several ideas have been pursued in retaining the accuracy associated with state-of-the-art CFD models while reducing model size and computational cost. Dynamically linear approximations are considered when the shock motion or the flow separation point is linearly proportional to the motion of the structure. This is sufficient to assess the linear stability of the aeroelastic system but not to determine LCO amplitudes due to nonlinear aerodynamic effects (Fusi *et al.* 2013). Frequency-domain analysis can be used to create reduced order computational models from higher order nonlinear CFD codes. The classical Describing Function (DF) technique falls under this class of methods; it requires the quasi-linearization of nonlinearities of the aeroelastic system (Gelb and Velde 1968).

The current study is focused on a comprehensive investigation of the role of shock wave dynamics in non-classical aileron buzz using CFD simulations. A numerical model based on CFD is used to develop a quasi-linear approximation of the nonlinear aerodynamic forces using the describing function, which allows the prediction of LCO characteristics while retaining the accuracy associated with CFD models. Unlike the approach employed by (He *et al*. 2016), the DF used in this work is a Multiple Input Describing Function (MIDF) to take into account the dependence of the LCO characteristics from the bias term introduced by the trim condition about which the oscillation is developed (Manetti, Quaranta and Mantegazza 2009). This research effort will be presented as follows: Section 2 will present an overview of the numerical model based on CFD while section 3 will analyze the results obtained from this numerical model. Section 4 will detail the development of the aerodynamic describing function and a comparative analysis of the results when the CFD model is replaced by the DF representation.

2. Numerical model

To accurately solve this non-linear aeroelastic problem, it is necessary to use sophisticated mathematical models and numerical methods from the very active research field of computational aeroelasticity. The main features of the aeroelastic system of aileron buzz are highlighted by the analogy to control theory presented in the block diagram sketched in Fig. 2(a). The aeroelastic computational model used in the current study is the result of the coupling between the structural degrees of freedom (I) of the aileron, namely the aileron deflection angle β and the aerodynamic model (A) which gives the aerodynamic load acting on the control surface, namely the hinge moment M_H. The dynamic model is represented by a 2D asymmetrical airfoil with a control surface. The latter is hinged at the three-quarter-chord location and its rotation about the hinge is modeled as rigid. The positive deflection angle of the aileron and hinge moment are shown in Fig. 2(b).
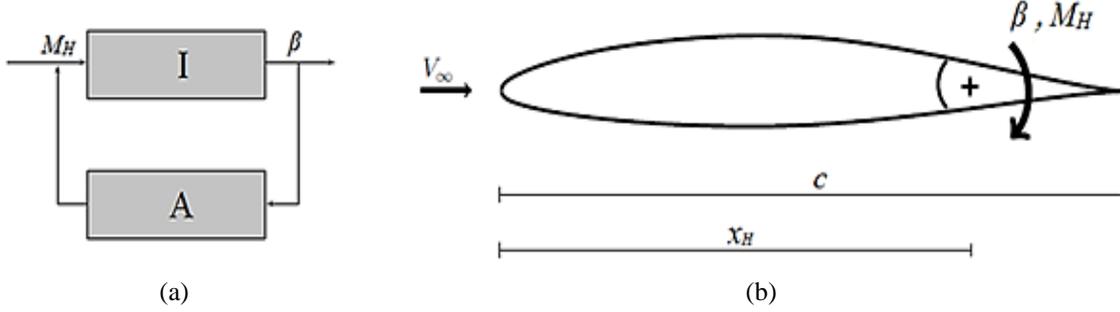
Fig. 2 Dynamic system

2.1 Aerodynamic model

In order to accurately study nonlinear aerodynamic effects for a buzz of Type B, a CFD numerical model based on Euler equation is used. This model is capable of representing the shock wave dynamics, which drive the instability in the case of non-classical aileron buzz, while it is not able to represent the boundary layer and so potential flow separations caused by shock-boundary layer interactions. Hence, it can only be used to study non-classical (type B) buzz for which flow separation does not appear to be the driving mechanism of instability. The simulation of aileron buzz requires the computation of an unsteady flow field for which the computational domain is continuously changing its shape to account for the control surface motion. Therefore it is necessary to resort to the Arbitrary Lagrangian Eulerian (ALE) formulation of the Euler equations

$$\frac{d}{dt} \int_{\Omega(t)} \mathbf{u} \, d\Omega + \oint_{\Gamma(t)} [\mathbf{f}(\mathbf{u}) - \mathbf{u}v] \cdot \boldsymbol{n} d\Gamma = 0 \tag{1}$$

that is completed by suitable initial and boundary conditions. $\Omega(t) \subseteq \mathbb{R}^2$ is the moving spatial domain and $\Gamma(t) = \partial\Omega(t) \subseteq \mathbb{R}$ represents the boundary having normal unit vector $\mathbf{n}(x,t)$ pointed outwards. Vector $\mathbf{u}(x,t)$ stores the unknown conservative variables, i.e., density, momentum and total energy, while vector $\mathbf{f}(\mathbf{u})$ includes the inviscid flux functions and vector $v(t)$ represents the local velocity of all the moving boundaries (Donea 1983). The finite volume discretization in space of Eq. (1) yields a set of ordinary differential equations in time, whose solution provides the pressure field around the wing section and thereby the time-varying aerodynamic moment acting on the aileron (Isola *et al.* 2015). For numerical implementation, the *AeroFoam* solver is used, whose development started back in 2008 and continues today (Romanelli *et al.* 2010). The aerodynamic grid is a C-mesh built around the wing section and it is smoothly refined in a radial sense from the far-field boundary to the body and around the hinge line.

2.2 Structural model

The structural model is represented by a rigid aileron integrated into the two dimensional wing section. Aileron motion is described by single degree of freedom motion about its hinge, namely aileron deflection angle $\beta(t)$, with the governing equation for dynamics of structural model given as

$$I_H \ddot{\beta}(t) = M_H(t) \tag{2}$$

where I_H is the aileron moment of inertia and $M_H(t)$ is the aerodynamic moment acting on the aileron, both evaluated with respect to the hinge line. Eq. (2) provides the balance between inertial and aerodynamic forces, while structural elastic and dissipative contributions are not modeled in the present work. Here a classical direct control chain with no servo-hydraulic system is modelled. For practical purposes, the addition of hinge stiffness or damping may provide ways of curing or reducing aileron buzz. In any case, the inclusion of elastic hinge stiffness would increase the aileron oscillation frequency and alleviate the buzz amplitude. Flight tests and experiments have shown that a limited aileron hinge stiffness (within reasonable limits) has little or no effect on the instability boundary, while significantly high values of stiffness may cure some types of buzz (Erickson and Stephenson 1947, Erickson and Mannes 1949). However, this is not always the case, as shown in the experimental work of (Parker *et al.* 1990). The primary goal of this work is to develop a reduced order model representation of nonlinear aerodynamics, therefore only the inertial terms have been retained in the structural dynamics and the elastic contribution of the structure has not been considered. As a matter of fact, the dynamic model of the aerodynamics provides damping and stiffness to the overall aeroelastic system and, indeed, it is the value of these aerodynamic elastic and dissipative contributions that tunes the energy exchange between the aerodynamic and structural sub-systems, resulting in stability or instability.

For the asymmetrical airfoil under consideration, the initial condition for the equation of motion is a perturbation provided by the initial steady unbalanced aerodynamic moment acting on the aileron while it is at zero-deflection angle. The aeroelastic interface is created exploiting the fact that the airfoil and the flap are rigid (Fusi *et al.* 2012). Hence, at each instant of time the aileron deflection angle is calculated and the displacements of the boundary cells surrounding the aileron are related to the aileron deflection angle through a rotation operator. The structural displacement and the velocity field are then translated into a variation in the boundary conditions of the aerodynamic subsystem through an aeroelastic interface operator.

The two dimensional NACA 65-213 airfoil used for the current study has been applied extensively to such aeroelastic problems, both in numerical simulations and wind tunnel tests (Lambourne 1958, Bendiksen 1993). This choice of airfoil is based on the availability of the necessary data for buzz simulation along with some historical perspectives available also for this airfoil. Th earliest observation of control surface buzz was established during flight tests of the P-80 jet fighter aircraft whose airfoil shape is similar to the NACA 65-213. Validation data was obtained from Howlett (1992), for the following airfoil parameters: airfoil chord c=1.472 m, aileron moment of inertia $I_H = 0.5536 \, \mathrm{kg\,m^2}$ and Reynolds number $\mathrm{Re} = 1.10^7$.

3. Test and results

The reliability of the presented numerical model and problem setup has been extensively established by earlier research works (Romanelli *et al.* 2010, Fusi *et al.* 2012, Biganzoli and Quaranta 2009) through various tests and by tackling a set of realistic static and dynamic aeroelastic problems. A C-mesh with hexahedral elements is used to model the flow. It extends ±10 chords both chordwise and in the airfoil thickness direction. A convergence study reported in (Fusi *et al.* 2012) showed that with about 50000 elements it is possible to reach a sufficient degree of spatial convergence.

For the current problem setup, responses computed at various Mach numbers and angles of attack show a pattern of buzz appearance after unrestrained motion, once set free from the initial
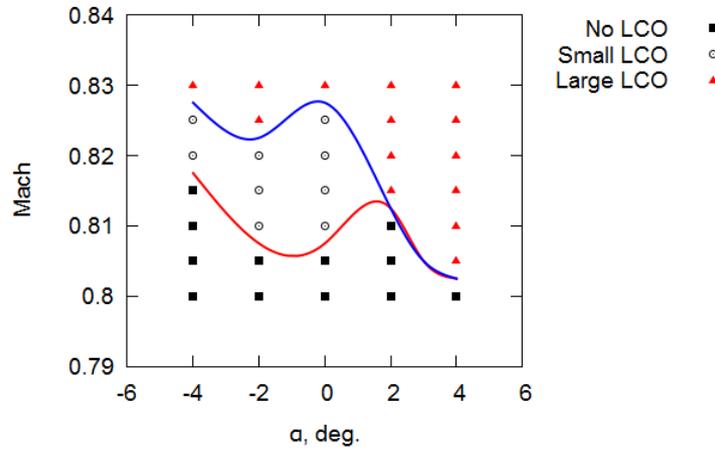
Fig. 3 LCO map in the mach angle of attack plane. Lines separate the regions of no LCO, small LCO and large LCO amplitudes
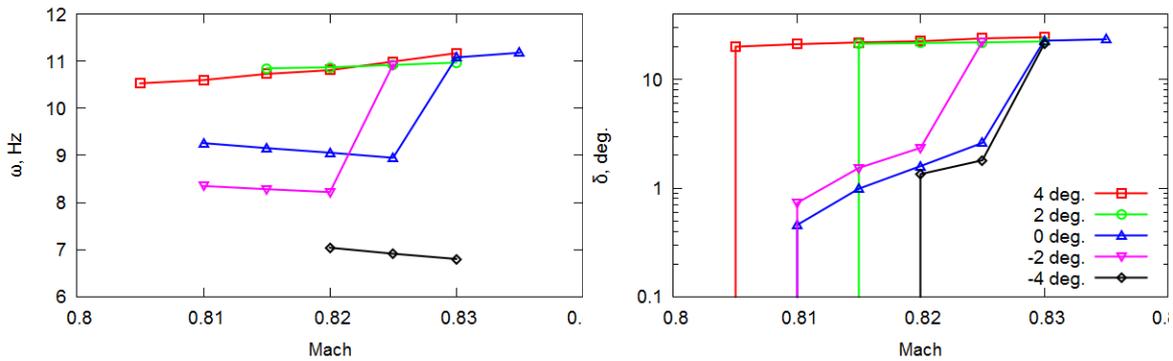

Fig. 4 LCO frequency (ω) and amplitude (δ) (logarithmic scale) variation

condition $\beta = 0$. Fig. 3 shows the set of Mach numbers and angles of attack that lead to small or large amplitude limit cycle oscillations under the prescribed initial conditions. Due to the asymmetric shape of the wing section, the appearance of large limit cycle oscillations can be observed at lower Mach numbers for positive angles of attack and at higher Mach numbers for negative angles of attack.

Further knowledge of LCO characteristics at these points, especially of the amplitude of oscillation, is of critical importance. Fig. 4 shows the variation of these characteristics where outburst in limit cycle amplitude can be observed along with corresponding increases in frequency. Further insight into this intriguing nature of interaction between shock wave dynamics and aileron unrestrained motion will aid in formulating the interplay between the wing section's asymmetric shape, relative shock wave motion and the resulting LCO characteristics.

Fig. 5 plots the spatial movement of the shock waves with increasing Mach number for the case of the airfoil at zero angle of attack. For Mach numbers just above the critical value, the equilibrium shock positions are affected solely by the camber of the airfoil. So, the upper shock is ahead of the lower shock even when the aileron has negative (upwards) deflection for zero hinge-
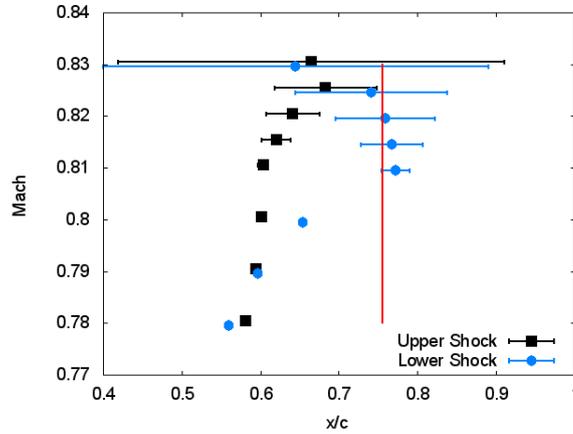
Fig. 5 Spatial variation of upper shock and lower shock for AOA=0 deg; Hinge location represented by red line. The dots represent the mean point of the oscillation amplitude or the stationary position of the shock when no LCO is present
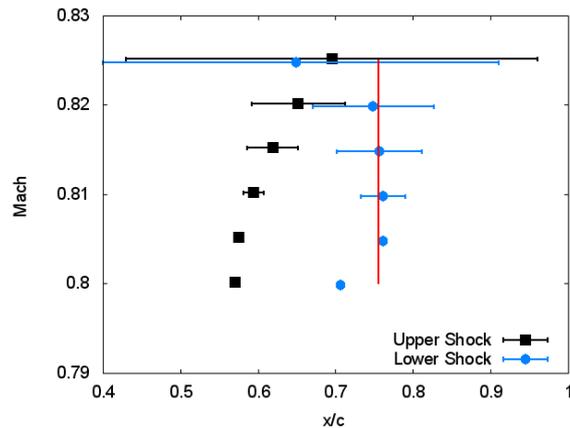

Fig. 6 Spatial variation of upper shock and lower shock for AOA=-2 deg; Hinge location represented by red line. The dots represent the mean point of the oscillation amplitude or the stationary position of the shock when no LCO is present

moment. As Mach number increases, and consequently shocks move closer to the aileron, shock positions are also effected by aileron negative (upwards) deflection with lower shock settling ahead of the upper shock. As long as aileron can settle to trim mean deflection for zero-hinge moment without locating shock waves on its surface, buzz is not excited. Further increase in Mach number results in aileron interaction with moving shock waves so that energy is extracted from the flow and buzz ensues.

The amplitude of oscillation increases with increasing Mach number. However, the critical information is the condition when this amplitude escalates to very high values. Careful observations show that this phenomenon occurs when either increase in Mach number or geometrical effects causes both the upper and lower shock waves to partially move across the aileron hinge. From Fig. 5, it is evident that until *M*=0.825, the upper shock has not started moving
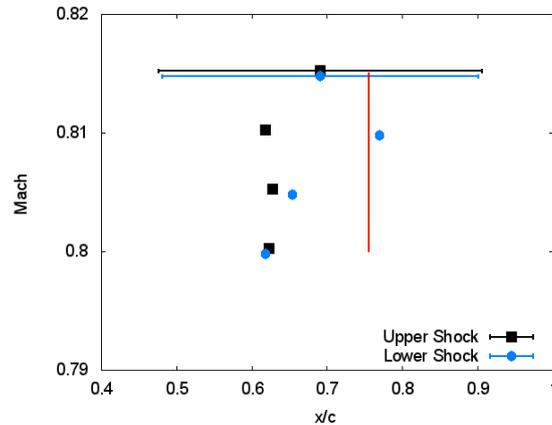
Fig. 7 Spatial variation of upper shock (US) and lower shock (LS) for AOA=+2 deg. Hinge location represented by red line. The dots represent the mean point of the oscillation amplitude or the stationary position of the shock when no LCO is present

over aileron so that the LCO amplitude is of lower amplitude. However, a further increment in Mach number (i.e., M=0.83) causes the upper shock to move onto the aileron leading to a jump in oscillation amplitude. Similar conclusions can be drawn from Fig. 6, where results computed at an angle of attack of -2 degrees show that the amplitude remains low until the upper shock also starts interacting with the aileron by partially moving over it, along with the lower shock.

Spatial variation of shock waves for an angle of attack of +2 degrees, shown in Fig. 7, represents either the condition of no limit cycle oscillation or that of very high amplitude. The buzz phenomenon in this case is being strongly effected by geometrical effects, which was not the case for lower angles of attack. Simulations have shown the appearance of expansion waves due to the geometrical edge appearing on the lower surface at the hinge location during the upwards aileron deflection. Rapid pressure change to lower value caused by these expansion waves at hinge location results in increasing the intensity of shock wave ahead of the hinge to recover pressure to higher values. This added intensity of shock wave due to geometrical effects leads to more energy being imparted by the fluid to the structure compared to the energy that would have been imparted in the absence of geometrical edge under similar flow conditions. The net effect is the appearance of high amplitude buzz at relatively low Mach number compared to the cases at lower angles of attack.

The amplitude jump can be understood by studying the time lag between the aerodynamic moment due to the unsteady pressure distribution and the structural displacement. This time lag can lead to higher values of negative aerodynamic damping.

To emphasize this point, instantaneous pressure coefficient C_P distributions are plotted in Fig. 8 at two instants in time, corresponding to two different values of aileron deflection. When a shock wave is located on the aileron, part of the aileron is exposed to supersonic flow with very low pressure coefficient, hence a significant net moment acts on the aileron. At time instant 0.11 s, the aileron is moving upwards, while a shock lying on its upper surface pushes it in the direction of motion. The situation is reversed at time instant 0.15 s, when the aileron is moving downwards and a shock lies on its lower surface, pushing it again in the direction of motion. This mechanism leads to a significant increase in amplitude and potentially fatal oscillations in very few cycles.
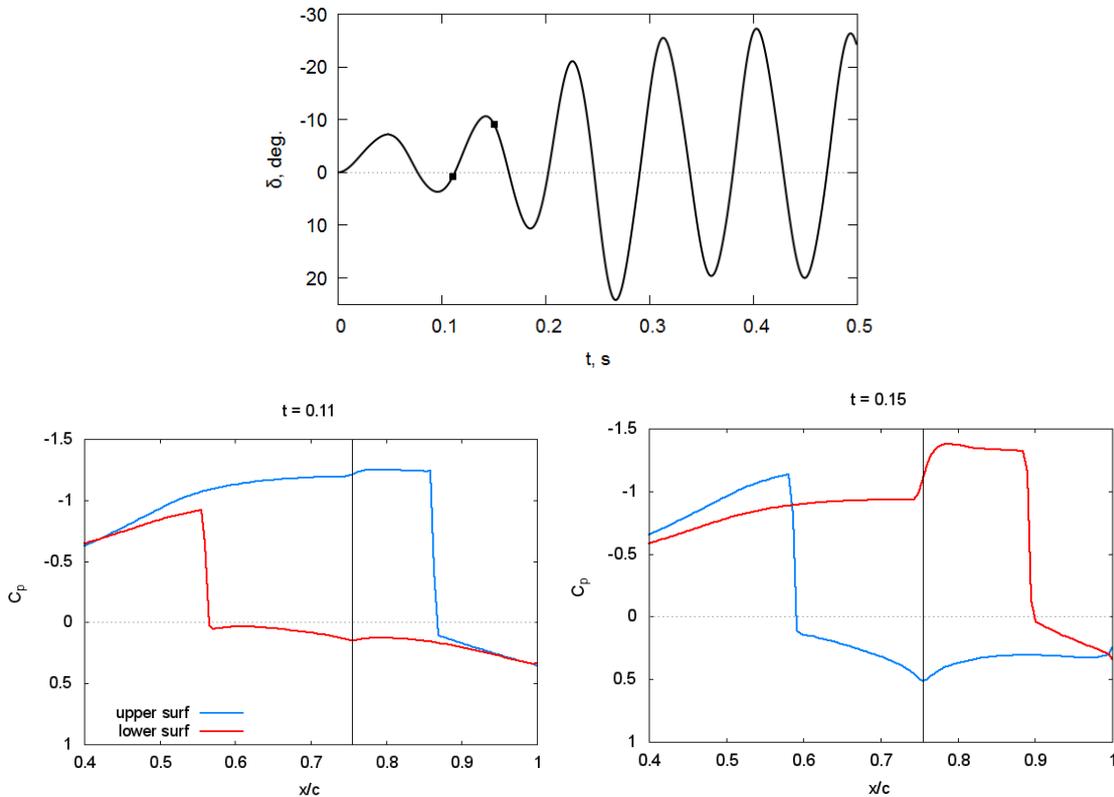
Fig. 8 Momentary relation between aileron motion and shock location

On the basis of the above discussion, it can be clearly inferred that the shape of the airfoil will affect the shock waves' location and consequently the buzz development. For a symmetrical airfoil at zero angle of attack, upper and lower shock waves would move symmetrically towards the trailing edge with increasing Mach number, which means that at zero aileron deflection there would be zero initial disturbance. Hence, for the cases where shock waves have not reached the aileron's surface, buzz would not be excited unless some significant initial disturbance is provided. At certain Mach numbers, the upper and lower shock waves would reach aileron surface simultaneously, leading to oscillations of high amplitude, as discussed in the preceding paragraphs. Hence the conditions for small amplitude Limit Cycle Oscillation due to the motion of only one shock wave over the aileron surface cannot exist for symmetrical airfoils at zero angle of attack. However at non-zero angle of attack small amplitude LCOs could arise with shock waves now moving asymmetrically. This inference is supported by the computational results presented by Bendiksen for the symmetrical airfoil NACA 64A006 where high amplitude self-induced oscillations were induced where the two shock waves moved symmetrically (Bendiksen 1993).

The results discussed above justify the occurrence of buzz with respect to the shock waves' relative motion. Buzz characteristics have been found to be highly dependent on initial flow perturbation and, hence, the initial displacement of the aileron from its mean position. In addition, geometrical aspects like the asymmetrical shape of the wing section and edge appearance on the airfoil's surface have significant effects.
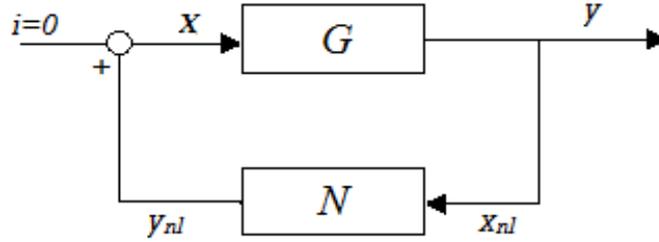
Fig. 9 Quasi-linearized system

4. Aerodynamic describing function

The Describing Function (DF) technique provides a framework for approximating the nonlinear system under investigation by a quasi-linear model. This type of quasi-linear system retains the possibility of using some analysis methods typical of linear systems (Gelb and Velde 1968).

For DF to reproduce the overall nonlinear response, the linear part of the system should act as a low pass filter with passband low enough to rule out higher harmonics out of the response. This low-pass filtering hypothesis is usually verified but it is rarely possible to check it up front, and so the DF method is often considered an empiric approach.

The approximation of the aerodynamic subsystem nonlinearity by a describing function is demonstrated in Fig. 9, which represents the aeroelastic system as a feedback loop where the linear element, i.e., the structural subsystem, is characterized by its frequency response function $G(j\omega)$ and the nonlinear element, i.e., the aerodynamic subsystem, is characterized by its DF $N(\omega, \delta, \gamma)$ representation.

The structural subsystem $G(j\omega)$ takes the aerodynamic moment as input and outputs the aileron deflection angle. The frequency response function for this linear element can be written as

$$G(j\omega) = \frac{\beta(j\omega)}{M_H(j\omega)} = -\frac{1}{I_H \omega^2} \tag{3}$$

Eq. (3) shows that the structure is a clear a low-pass filter given its dependence on the inverse of the square of the natural frequency.

For oscillatory behavior of an asymmetrical airfoil, a sinusoidal signal plus a bias can be considered as an appropriate form for the flap rotation when in LCO conditions

$$x_{nl}(t) = \gamma + \delta \sin(\omega t) \tag{4}$$

which has a bias component γ and a sinusoidal component with frequency ω and amplitude δ. The values of γ, δ and ω are determined by the nature of the system and its inputs. The output of the aerodynamic block, i.e., the hinge moment, can be expressed by using a Fourier series

$$y_{nl}(t) = \sum_{n=0}^{\infty} |A_n(\omega, \delta, \gamma)| \ \sin[n\omega t + \phi(\omega, \delta, \gamma)]$$

where A_n are Fourier coefficients. Such coefficients are functions of input frequency, bias and amplitude because they describe the output of a nonlinear element. The nonlinear output can be further decomposed into the form
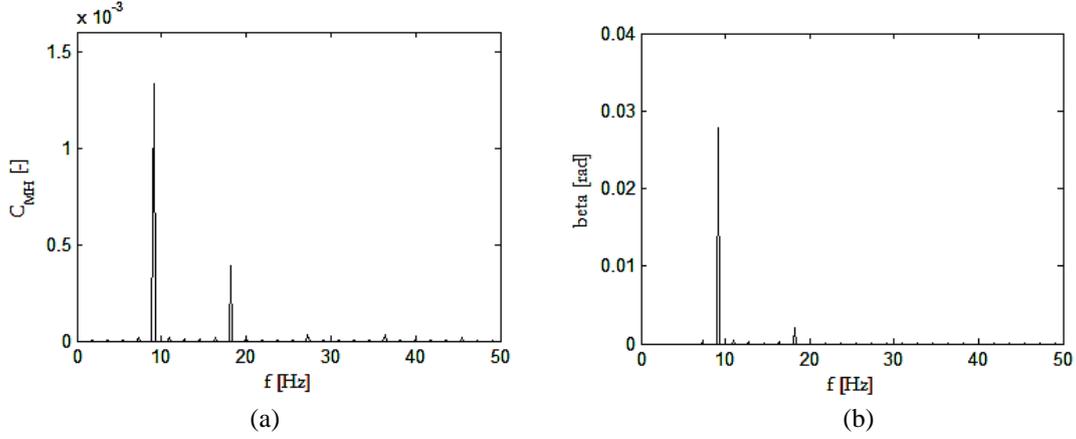
Fig. 10 Frequency spectrum output of aerodynamic subsystem (a) and output of structural subsystem (b) for free oscillation

$$y_{nl}(t) = y_a(t) + y_r(t)$$

where $y_a(t)$ contains the contributions of the constant and fundamental frequency terms ($n = 0, 1$) and $y_r(t)$ denotes the contributions of higher harmonics ($n > 1$). The output after passing through the linear element, takes the form as:

$$y(t) = G.y_a(t) + G.y_r(t)$$

The low-pass filtering of the structural block is here verified through the simulation of free oscillation responses. The frequency spectrum for free oscillation is shown in Fig. 10. A significant second harmonic can be observed in the aerodynamic subsystem response (Fig. 10(a)), which is significantly attenuated by the linear structural subsystem (Fig. 10(b)).

Hence under this important filtering approximation, higher harmonic contributions can be neglected as:

$$G.y_a(t) \gg G.y_r(t)$$

Consequently, the nonlinear output of the aerodynamic block can be approximated by considering only the first harmonic term plus bias, neglecting the higher harmonics. The following form of the Dual Input Describing Function is obtained

$$y_a(t) = N_\gamma \gamma + [\,\Re[N_\delta] \sin(\omega t) + \Im[N_\delta] \cos(\omega t)\,]\,\delta \qquad (5)$$

where N_γ and N_δ are approximating gains to bias and sinusoidal input components respectively and are given as

$$N_\gamma(\omega, \delta, \gamma) = \frac{A_0(\omega, \delta, \gamma)}{\gamma} \qquad (6)$$

and

$$N_\delta(\omega, \delta, \gamma) = \frac{|A_1(\omega, \delta, \gamma)|}{\delta} e^{j\varphi(\omega, \delta, \gamma)} \qquad (7)$$

while $\Re[.]$ represents the real part of a complex number and $\Im[.]$ is the imaginary part. N_δ is generally defined as the complex fundamental-harmonic gain of a nonlinearity in the presence of a driving sinusoid. The coefficients of Eqs. (6)-(7) will be evaluated through several direct time marching simulation with the CFD model for different values of the input parameters, i.e., γ, δ and ω. Then a cubic spline interpolation is used to obtain the value for any input parameter combination.

The complete quasi-linearized aeroelastic system output can be formulated as:

$$y(t) = Gy_{nl}(t) \cong Gy_a(t)$$

$$y(t) \cong G(j0)N_\gamma.\gamma + (\Re[G(j\omega)] \{\Re[N_\delta]\sin(\omega t) + \Im[N_\delta]\cos(\omega t)\}$$

$$+ \Im[G(j\omega)] \{\Re[N_\delta]\sin(\omega t) + \Im[N_\delta]\cos(\omega t)\}) \delta$$

At the limit cycle condition, $y(t) = x_{nl}(t)$, which leads to following set of equations

$$G(j0)\, N_\gamma(\omega, \delta, \gamma)\, \gamma = \gamma \tag{8}$$

$$G(j\omega)\, \{\Re[N_\delta]\sin(\omega t) + \Im[N_\delta]\cos(\omega t)\}\, \delta = \delta\sin(\omega t) \tag{9}$$

The two equations above define the conditions necessary for limit cycles to occur. For non-zero mean ($\gamma \neq 0$) and static gain $G(j0) \to \infty$ (see Eq. (3))

$$N_\gamma(\omega, \delta, \gamma) = 0 \tag{10}$$

which gives the condition for the bias value necessary to sustain a limit cycle. Eq. (9), can be further decomposed into

$$G(j\omega)\,.\,\Re[N_\delta(\omega, \delta, \gamma)] = 1 \tag{11}$$

$$G(j\omega)\,.\,\Im[N_\delta(\omega, \delta, \gamma)] = 0 \tag{12}$$

Eqs. (10)-(12) form the set of three real nonlinear algebraic equations that must be solved for the three unknown parameters characterizing the limit cycle oscillations, which are bias, amplitude & frequency (Manetti *et al.* 2009).

The aerodynamic describing function is evaluated numerically through simulations at several Mach numbers, angles of attack, frequencies, γ and δ values. Table 1 shows the range of values considered. The variation of the real (Eq. (11)) and imaginary components (Eq. (12)) of the complex fundamental harmonic gain (N_δ) with frequency (ω), angle of attack and Mach number
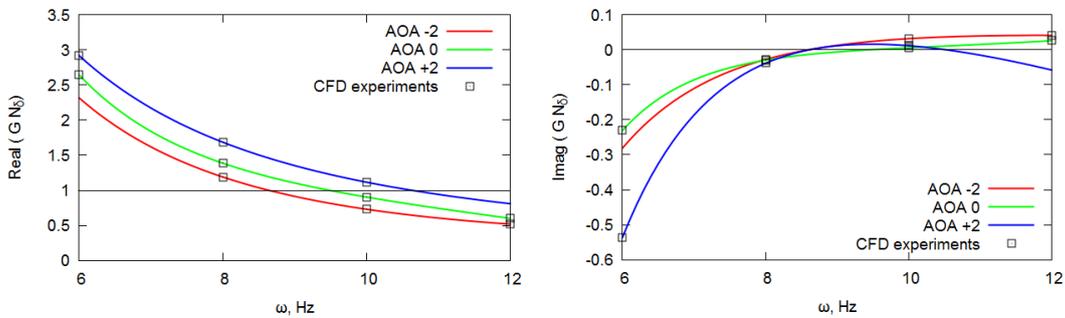

Fig. 11 Variation of real and imaginary components of complex harmonic gain N_δ w.r.t frequency (ω). Mach 0.82, γ=-4deg, δ=20 deg. And variable angle of attack
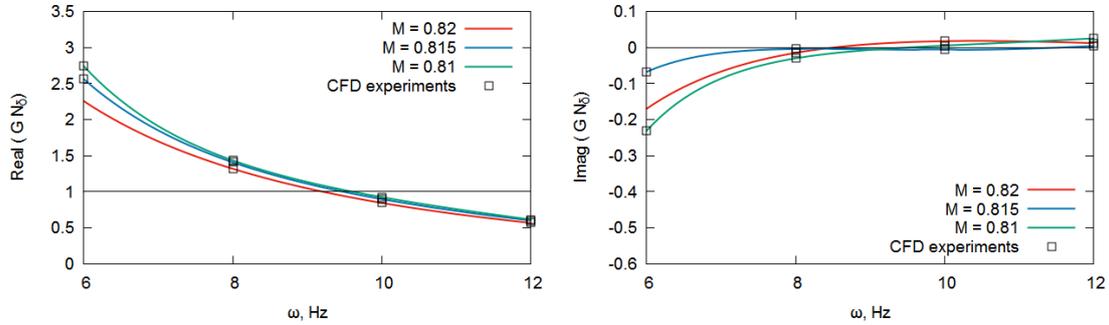
Fig. 12 Variation of real and imaginary components of complex harmonic gain N_δ w.r.t frequency(ω). Angle of attack 0 deg, γ=-4 deg, δ=20 deg and variable Mach number

Table 1 Range of variables used for the identification of the aerodynamic describing function through CFD simulation

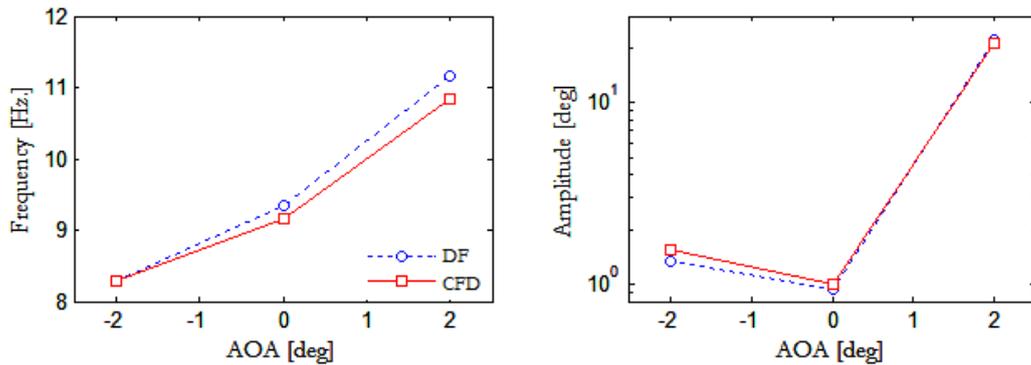| Mach	AOA, deg	Frequency, Hz	Bias, deg	Amplitude, deg
0.81, 0.815, 0.82	-2, 0, +2	6, 8, 10, 12	-6, -4, -2, 0	[0.5 - 3.5]

Fig. 13 Aeroelastic system response comparison at mach no. 0.815

is shown in Figs. 11-12. Convergence to an LCO condition is achieved the two components are equal to 1 and 0 respectively, along with the satisfaction of Eq. (10).

While complex harmonic gain is a function of three variables, frequency, amplitude and mean, and its variation is non-linear, a single convergence point for the solution of this set of equations could not be achieved by directly analyzing the cubic spline functions' variation. Minimum error points were evaluated for each case through iteratively calculating the left hand side terms of the Eq. (10)-(12). These minimum error points were further analyzed with respect to the amount of error attached to each point (highest weighting to the point with least error) to arrive at a single point providing the characteristics of LCOs.

In this way, using the evaluated aerodynamic describing functions and interpolating them using multidimensional cubic splines, a DF linearized aeroelastic system was formulated to predict LCO parameters and their variation with reasonable accuracy compared to the ones computed through CFD-based aeroelastic computations. Figs. 13-14 show the comparisons of the predicted
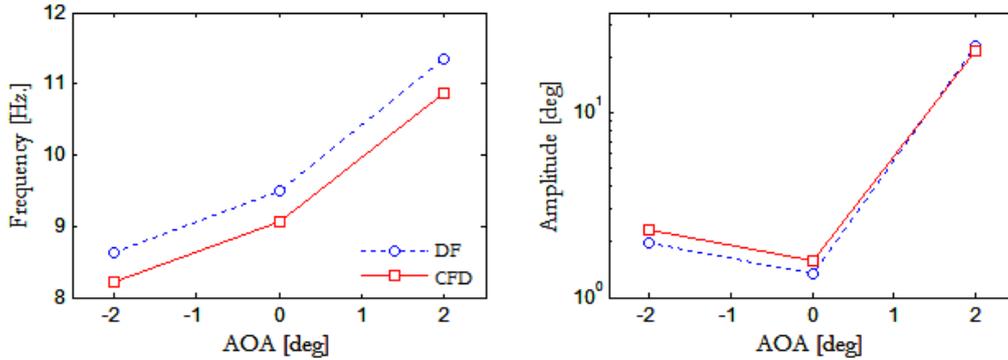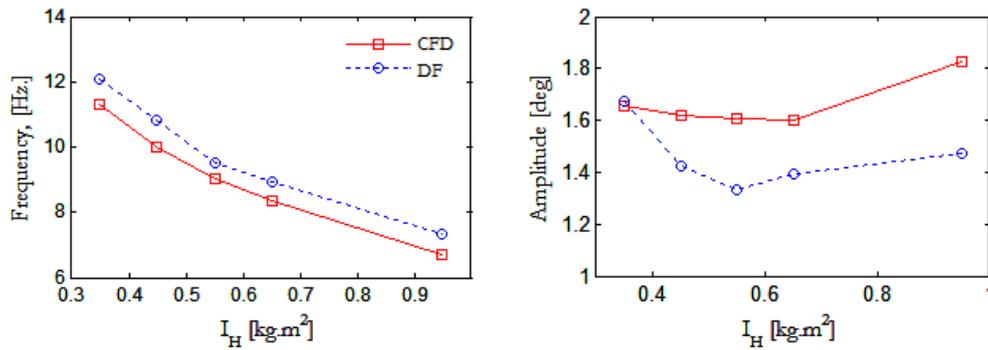
Fig. 14 Aeroelastic system response comparison at mach no. 0.82

Fig. 15 LCO characteristics variation with hinge moment of inertia (I_H)

oscillation parameters at several angles of attack. The DF linearized aeroelastic system predicts the variation of these parameters with good accuracy and with little discrepancy for the CFD values. These results show the potential of the describing function technique for developing reduced order representations of aerodynamic nonlinearity.

The linearized aeroelastic system should also be able to predict the variation of LCO characteristics with respect to design variables, which in the present case is the hinge moment of inertia. This verification has been performed and the results are shown in Fig. 15. Significant variation in limit cycle frequency is observed with respect to hinge moment of inertia and this variation has been predicted with good accuracy. The limit cycle amplitude has been under-predicted but its dependence on hinge moment of inertia is low relative to the frequency. These results demonstrate that the describing function technique is a powerful approach for non-linear aerodynamic modeling and predicting the characteristics of limit cycle oscillations.

5. Conclusions

This work investigated the nonlinear interaction between aileron unrestrained oscillation and shock wave dynamics, which is the driving mechanism for non-classical aileron buzz. Simulation

results give a detailed insight into the interplay between wing section geometry, shock wave motion with respect to various flow conditions and excitation of aileron buzz. The characteristics of the resulting oscillations have been found to be highly dependent on shock wave position and geometrical aspects of the wing section, especially in relation to asymmetry and edge appearance on the airfoil. Furthermore, the classical Describing Function technique has been used to develop a quasi-linearized representation of the aerodynamics nonlinearities involved in non-classical aileron buzz. The resulting DF linearized aeroelastic system predicts limit cycle oscillation characteristics with satisfactory accuracy.

References

Bendiksen, O.O. (1993), "Nonclassical aileron buzz in transonic flow", *Proceedings of the 34th AIAA(ASME/ASCE/AHS/ASC Structures, Structural Dynamics and Materials Conference, AIAA/ASME Adaptive Structures Forum, AIAA 93-1479*, La Jolla, California, U.S.A.

Biganzoli, E. and Quaranta, G. (2009), "Nonlinear reduced order models for aileron buzz", *Proceedings of the International Forum on Aeroelasticity and Structural Dynamics*, Seattle, U.S.A.

Donea, J. (1983), *Arbitrary Lagrangian-Eulerian Finite Element Methods*, Computational Methods for Transient Analysis, Amsterdam, The Netherlands: Elsevier Science Publisher, 474-516.

Erickson, L. and Jack, D. (1947), "A suggested method of analyzing for transonic flutter of control surfaces based on available experimental evidence", California: Ames Aeronautical Laboratory.

Erickson, L. and Robert, L. (1949), "Wind-tunnel investigation of transonic aileron flutter", Washington: National Advisory Committee for Aeronautics.

Forestieri, G., Guardone, A., Isola, D., Marulli, F. and Quaranta, G. (2011), "Numerical simulation of aileron buzz using an adaptive-grid compressible flow solver for dynamic meshes", *Proceedings of the 4th International Conference on Computational Methods for Coupled Problems in Science and Engineering*, *Coupled Problems*, Ischia, Italy.

Fuglsang, D.F., Brase, L.O. and Agrawal, S. (1992), "A numerical study of control surface buzz using computational fluid dynamic methods", *Proceedings of the 10th Applied Aerodynamics Conference*, California, U.S.A.

Fusi, F., Romanelli, G., Guardone, A. and Quaranta, G. (2012), "Assessment of geometry reconstruction techniques for the simulation of non-classical aileron buzz", *Proceedings of the ASME International Mechanical Engineering Congress and Exposition*, Houston, Texas, U.S.A.

Fusi, F., Romanelli, G., Guardone, A. and Quaranta, G. (2013), "Nonlinear reduced order models of unsteady aerodynamics for non-classical aileron buzz analysis", *Proceedings of the International Forum on Aeroelasticity and Structural Dynamics*, Bristol, United Kingdom.

Gao, C.Q., Wei-Wei, Z., Yi-Lang, L., Zheng-Yin, Y. and Yue-Wen, J. (2015), "Numerical study on the correlation of transonic single-degree-of-freedom flutter and buffet", *Sci. China Phys. Mech. Astron.*, **58**(8), 1-12.

Gelb, A. and Velde, W.E.V. (1968), *Multiple-Input Describing Functions and Nonlinear System Design*, McGraw-Hill Book Company.

He, S., Zhichun, Y. and Yingsong, G. (2016), "Limit cycle oscillation behavior of transonic control surface buzz considering free-play nonlinearity", *J. Fluid. Struct.*, **61**, 431-449.

Howlett, J.T. (1992), *Calculations of Unsteady Transonic Flows with Mild Separation by Viscous-Inviscid Interaction*, Hampton, Virginia: NASA Langley Research Center.

Isola, D., Guardone, A. and Quaranta, G. (2015), "Finite-volume solution of two-dimensional compressible flows over dynamic adaptive grids", *J. Comput. Phys.*, **285**, 1-23.

Lambourne, N.C. (1958), "Some instabilities arising from the interactions between shock waves and boundary layers", Tech. Rep., No. AGARD-182.

Lambourne, N.C. (1962), "Control-surface buzz", *HM Station. Office*, 3364.

Manetti, M., Giuseppe, Q. and Paolo, M. (2009), "Numerical evaluation of limit cycles of aeroelastic system", *J. Aircraft*, **46**(5), 1759-1769.

Pak, C. and Baker, M. (2001), "Control surface buzz analysis of a generic NASP wing", *Proceedings of the 42nd AIAA/ASME/ASCE/AHS/ASC Structures, Structural Dynamics, and Materials Conference and Exhibit*, Washington, U.S.A.

Parker, E.C., Spain, C.V. and Soistmann, D.L. (1990), "Experimental transonic buzz characteristics of a clipped delta-wing model with full span aileron", CR-1083, NASA.

Romanelli, G., Serioli, E. and Mantegazza, P. (2010), "A 'free' approach to computational aeroelasticity", *Proceedings of the 48th AIAA Aerospace Sciences Meeting*, Orlando, Florida, U.S.A.

Saito, H. (1959), "On the aileron buzz in transonic flow", Aeronautical Research Institute, University of Tokyo.

Steger, J.L. and Bailey, H.E. (1980), "Calculation of transonic aileron buzz", *AIAA J.*, **18**(3), 249-255.